Prevention of photoreceptor cell loss in a *Cln6*^{nclf} mouse model of Batten disease requires *CLN6* gene transfer to bipolar cells

Sophia-Martha kleine Holthaus[1,2], Joana Ribeiro[1], Laura Abelleira-Hervas[1], Rachael A Pearson[1], Yanai Duran[1], Anastasios Georgiadis[1], Robert D Sampson[1], Matteo Rizzi[1], Justin Hoke[1], Ryea Maswood[1], Selina Azam[1], Ulrich F O Luhmann[1,3], Alexander J Smith[1], Sara E Mole[2,4,5*] and Robin R Ali[1,6*]

[1]*Department of Genetics, UCL Institute of Ophthalmology, 11-43 Bath Street, London EC1V 9EL, UK*

[2]*MRC Laboratory for Molecular Cell Biology, University College London, Gower Street, London WC1E 6BT, UK*

[3]*present address: Roche Pharmaceutical Research and Early Development, Translational Medicine Neuroscience & Biomarkers, Roche Innovation Center Basel, Switzerland*

[4]*UCL Institute of Child Health, 30 Guilford St, London WC1N 1EH, UK*

[5]*UCL Department of Genetics, Evolution and Environment, University College London, Gower St., London WC1E 6BT, UK*

[6]*NIHR Biomedical Research Centre at Moorfields Eye Hospital NHS Foundation Trust and UCL Institute of Ophthalmology, City Road, London EC1V 2PD, UK*

[*]*These authors equally contributed to this work*

To whom correspondence may be addressed: s.mole@ucl.ac.uk or r.ali@ucl.ac.uk

Abstract

The neuronal ceroid lipofuscinoses (NCLs) are inherited lysosomal storage disorders characterised by general neurodegeneration and premature death. Sight loss is also a major symptom in NCLs, severely affecting the quality of life of patients but is not targeted effectively by brain-directed therapies. Here, we set out to explore the therapeutic potential of an ocular gene therapy to treat sight loss in NCL due to a deficiency in the transmembrane protein CLN6. We found that although *Cln6*^{nclf} mice presented mainly with photoreceptor degeneration, supplementation of CLN6 in photoreceptors was not beneficial. Because the level of *CLN6* is low in photoreceptors, but high in bipolar cells, retinal interneurons that are only lost in *Cln6*-deficient mice at late disease stages, we explored the therapeutic effects of delivering *CLN6* to bipolar cells using AAV serotype 7m8. Bipolar cell-specific expression of *CLN6* slowed significantly the loss of photoreceptor function and photoreceptor cells. This study shows that the deficiency of a gene normally expressed in bipolar cells can cause the loss of photoreceptors and that this can be prevented by bipolar cell-directed treatment.

Introduction

The neuronal ceroid lipofuscinoses (NCLs) are rare, inherited lysosomal storage disorders that present with severe neurodegeneration and sight loss. This group of diseases is more commonly referred to as Batten disease and at least 13 genes have been linked to the development of this condition with a combined incidence in different countries of between 1:12,500 and 1:100,000[1]. The affected genes code either for a soluble lysosomal protein or a transmembrane protein[2]. The development of therapies for forms of NCL caused by defects in lysosomal enzymes is aided by lysosomal cross-correction, which allows the therapeutic enzyme to be taken up by cells from the circulation and other cells via the mannose-6-phosphate pathway[3]. This phenomenon has helped to pave the way towards clinical trials for CLN2 disease, a common form of NCL arising from the deficiency in the lysosomal enzyme TPP1 (NCT01907087). Cross-correction, however, does not occur for transmembrane proteins, limiting functional restoration to individual cells and increasing the challenge to achieve a therapeutic effect.

CLN3 disease with juvenile onset is the most common form of NCL that is caused by a defect in a membrane-bound protein[4]. Other rarer forms caused by transmembrane protein deficiencies include CLN6, CLN7 and CLN8 disease, all variant forms with typically a late-infantile onset and a more rapid progression than CLN3 disease. NCLs usually manifest with seizures, visual decline resulting in blindness, progressive psychomotor and cognitive deteriorations. The order of the symptoms varies, yet these conditions collectively lead to premature death[5]. A major obstacle to developing brain-directed therapies for NCLs arising from transmembrane protein defects is the challenge to deliver agents throughout the brain. Recently, the partial rescue of the brain

phenotype in a CLN3 disease mouse model was described following brain-directed adeno-associated virus (AAV)-mediated gene therapies[6,7]. No correction of the disease pathology was reported outside of the brain underlining the need for treatments not only targeting the brain but also other affected organs like the eye. Moreover, ocular therapies may not only increase the quality of life of patients but may also help with the development of brain-directed treatments for NCLs.

Over the last decade, AAV-mediated gene therapies have been used for several animal models of monogenic retinal degenerations to restore the expression of soluble or transmembrane proteins and to treat vision loss[8-10]. These encouraging studies led to the commencement of clinical trials for inherited retinal degenerative conditions including Leber congenital amaurosis[11-13] and retinitis pigmentosa[14]. Here, we explored the therapeutic potential of an ocular AAV-mediated gene therapy in the *Cln6*^{nclf} mouse, a naturally occurring model of CLN6 disease, variant late-infantile. The mice carry a 1 bp insertion mutation in the *Cln6* gene which encodes a membrane-bound ER protein of unknown function[15]. The 1 bp insertion results in a frameshift and a truncated short-lived protein product and is also found in CLN6 patients of Pakistani origin[16,17]. *Cln6*^{nclf} mice present with loss of vision preceding severe neuropathological and behavioural abnormalities[18,19].

In this study we show that although retinal disease in *Cln6*^{nclf} mice is predominately characterised by photoreceptor degeneration, supplementation of *CLN6* in photoreceptors is not therapeutic. We also establish that in unaffected retinas, CLN6 is expressed in photoreceptors and bipolar cells but the level is much higher in bipolar cells. Although bipolar cells are only lost late in disease, AAV-mediated gene delivery

of *CLN6* to bipolar cells, leads to significantly increased retinal function and long-term preservation of photoreceptors. This study shows that photoreceptor degeneration can be prevented by treating bipolar cells.

Results

CLN6 *is more highly expressed in bipolar cells than in photoreceptors*

To determine the potential target cells for gene therapy, we investigated the endogenous expression of the *CLN6* gene in human and mouse retina. Due to the lack of antibodies against the murine protein we performed immunohistochemical stainings on human retina from non-diseased donor eyes using a previously reported antiserum against human CLN6[15]. We detected a weak fluorescent signal in the ONL and a strong fluorescent signal in the INL (Figure 1A, 1B, 1B''). In the INL the staining for CLN6 co-localised with staining for PKCα, demonstrating that rod bipolar cells express *CLN6* (Figure 1B, 1B', Figure S2A-B'). Co-staining with an antibody against CRALBP, a marker for Mueller glia cells, did not reveal any co-localisation (Figure S2A, S2A'). In the absence of antibodies that could be used for co-localisation with CLN6 staining, we were unable to determine what other cell types in the INL expressed the gene. Microarray data on the murine retina suggests that the remaining CLN6-positive cells are most likely to be other bipolar cell types, as rod bipolar cells only form a minor fraction of the retinal bipolar cell population[20].

Cln6^{nclf} mice have been reported to present with a predominant loss of photoreceptor function and photoreceptor cells[18,19]. We found that from postnatal day 21 (P21), retinal function in *Cln6*-deficient mice was progressively compromised under scotopic light conditions as measured by electroretinography (ERG) recordings (Figure S1A, S1C, S1D). The photopic ERG was unchanged (Figure S1B). Histological assessment and quantitative analyses of the outer nuclear layer (ONL) revealed no severe histological changes at P14 (Figure S1E, S1F). However, *Cln6*^{nclf} mice have a significantly reduced number of photoreceptor nuclei at 1 and 6 months compared with wild type controls (Figure S1G, S1H). The number of rod bipolar cells in the inner nuclear layer (INL)

was only reduced in mutant mice at 6 months ($p<0.001$) (Figure S1I, S1J). In line with previous reports these data show that *Cln6*^{nclf} mice suffer from an early but mildly progressing rod-mediated retinal degeneration, whilst loss of rod bipolar cells became only evident at late disease stages.

In the murine retina we assessed the expression of *Cln6* by quantitative real-time PCR (qRT-PCR). To confirm the expression of *Cln6* in murine photoreceptors and bipolar cells, we performed qRT-PCRs on mRNA obtained from fluorescence-activated cell sorted (FACS) photoreceptors, labelled with the cell surface marker CD73, and rod bipolar cells, labelled with td.tomato in a Pcp2.Cre/td.tomato mouse line (Figure S2B, S2C). In line with the staining on human retina, we found a trend with a higher expression level of *Cln6* in rod bipolar cells than in photoreceptors (Figure 1C). A direct comparison of the absolute number of mRNA molecules by qRT-PCR showed that *Cln6* was expressed to similarly high levels in whole mouse retina as the photoreceptor-specific gene *Peripherin2*, encoding a highly abundant retinal protein[21] (Figure 1D). We studied the relative expression level of *Cln6* in the retina over time using qRT-PCR and found that *Cln6* was expressed from birth to adulthood. From P0 to P14, a period when retinal cells undergo postnatal maturation leading to initiation of the phototransduction cascade and eye opening, the expression level of *Cln6* was relatively stable at around 50 % of adult levels. At P21 the expression level of *Cln6* increased to the level that was detected in adults (Figure 1E), which may indicate that *Cln6* could play a more important role during vision than during the ocular development.

AAV2/8-mediated supplementation of CLN6 in photoreceptors is not therapeutic in* Cln6^{nclf} *mice

We established that *CLN6* was expressed in photoreceptors and that *Cln6* deficiency led to severe loss of photoreceptors in mice, while no early death of bipolar cells was detected in *Cln6^{nclf}* mice despite the high endogenous expression level of *CLN6* in bipolar cells. Consequently, we set out to develop a gene supplementation therapy targeting photoreceptors and treated pre-symptomatic P9-P10 *Cln6^{nclf}* mice subretinally with an AAV2/8 vector carrying the ubiquitous CMV promoter and the human CLN6 (hCLN6) transgene (Figure S3). We administered three different doses ranging from $1.5x10^8$ vg/eye to $1.5x10^{10}$ vg/eye and performed ERG recordings at 1, 2, 4 and 6 months of age. As untreated *Cln6^{nclf}* mice presented with a progressive reduction in rod photoreceptor function, the main functional readout to assess whether the treatment was successful was the scotopic a-wave. None of the treated animals had significantly higher a-wave amplitudes than the untreated or AAV2/8.null vector-treated mutant animals at any time point (Figure 2A). Immunostaining confirmed the presence of the transgene at 6 months. In line with the ERG recordings, the ONL did not appear to be preserved in any of the treated eyes (Figure 2B-2D', Figure S1G). Further experiments targeting the photoreceptor cells, including earlier treatment at P5 and use of a weak photoreceptor-specific mouse opsin promoter[22], did not preserve photoreceptor function or improve photoreceptor survival. Since the human and mouse CLN6 protein share about 90% amino acid identity, we also assessed the efficacy of AAV8 carrying mouse Cln6 and a CMV promoter to exclude that slight differences in the amino acid sequence between human and mouse CLN6 could affect the outcome of the treatment. No treatment effect was observed (Table S1). These experiments demonstrated that an

AAV-mediated gene supplementation therapy targeting photoreceptor cells was not therapeutic in *Cln6*-deficient mice.

The AAV2/2 variant 7m8 transduces bipolar cells efficiently in wild type mice

Conventional AAV serotypes poorly transduce cells in the INL and bipolar cells are amongst the cell types least amenable to viral transduction[23]. Several studies have been undertaken to engineer AAV vectors to enhance their transduction efficiency or to increase cell type-specific transduction[24,25]. The recently developed AAV2/2 variant 7m8 was reported to penetrate the retina and transduce cells in all retinal layers following intravitreal delivery in adult mice[26]. To investigate the transduction efficiency of bipolar cells, we produced a 7m8 vector carrying eGFP under the CMV promoter. Wild type mice received intravitreal injections of the vector at P5, an age before the inner limiting membrane (ILM) is fully established. The ILM can act as a natural barrier in adult animals when AAVs are delivered intravitreally, preventing efficient penetration of viral particles into deep layers of the rodent retina[27,28]. Three weeks post injection we observed a widespread pan-retinal expression of eGFP (Figure 3A). Higher magnification images showed strongly transduced ganglion and Mueller glia cells as well as more sparsely transduced photoreceptors (Figure 3C). Immunostaining for PKCα and single confocal images revealed that several rod bipolar cells expressed eGFP (Figure 3B, 3C' white arrows). To visualise better the transduction of bipolar cells we injected wild type animals with a 7m8 vector carrying eGFP under the weak Purkinje cell protein 2 (PCP2) promoter[29] (Figure S4A, S4A') or the 4x enhanced Grm6 (Grm6) promoter[25] driving expression in rod bipolar cells or all ON bipolar cells, respectively. Magnified single images showed that the majority of PKCα-positive bipolar cells and several cone ON bipolar cells (arrow heads), contained eGFP (Figure 3D, 3E). We quantified the proportion of transduced bipolar cells following the administration of 7m8 by flow cytometry. PCP2.Cre/td.tomato mice received intravitreal injections with 7m8.CMV.eGFP at P5 or P6 and we found that

approximately 65 % of the td.tomato-positive rod bipolar cells were positive for eGFP (Figure 3F). We further analysed the number of transduced photoreceptors and established that approximately 25 % of the CD73-positive photoreceptors expressed eGFP (Figure S4B, S4C). Due to the lack of specific markers labelling all cone bipolar cells we did not quantify the transduction of other types of bipolar cells.

Intravitreal delivery of 7m8.CMV.hCLN6 slowed the loss of photoreceptor function and photoreceptor cells in* Cln6^{nclf} *mice

ERG recordings at 1 month following intravitreal injections of 7m8.CMV.hCLN6 in *Cln6^{nclf}* mice at P5 to P6, demonstrated that mutant eyes that received a vector dose of $1x10^{10}$ vg had significantly higher scotopic a-wave amplitudes than untreated eyes or eyes that received 7m8.null control vector. The ERG amplitudes decreased slightly but remained significantly higher in treated than in untreated or 7m8.null-treated eyes at 4, 6 and 9 months. Representative scotopic ERG traces of a mutant mouse that received $1x10^{9}$ vg of 7m8.CMV.hCLN6 in one eye and no treatment in the contralateral eye are shown in figure 4B, demonstrating the striking difference in retinal function between treated (red traces) and untreated (black traces) eyes at 9 months (see also Figure S5A, Table S2). Histological assessment of the treated eyes at 6 months confirmed the expression of human *CLN6* in cells of all retinal layers. Consistent with the ERG recordings, treated retinas had a thicker ONL, a better structure of photoreceptor OS and reduced activation of Mueller glia cells as indicated by DAPI, rhodopsin and GFAP staining, respectively (Figure 4C). Counts of DAPI-positive photoreceptor nuclei showed that the number of nuclei was higher with an average of 6 and 7 rows of nuclei in the low titre and high titre group compared with 4 rows in untreated mutant eyes (Figure 4D). At 6 months counts of PKCα-positive cells did not reveal any significant

changes between treated and untreated eyes (Figure 4E). Histological assessment at 9 months confirmed the long-term expression of the therapeutic transgene in treated retinas. It also was apparent that whilst the retinal degeneration continues to progress from 6 to 9 months resulting in 2 remaining rows of photoreceptor nuclei in *Cln6*-deficient mice, the number of photoreceptor nuclei was maintained following the 7m8 treatment with 6 and 7 rows of nuclei in the two treatment groups (Figure 4F, 4G). Similarly, the quantification of rod bipolar cells showed that untreated eyes continued to lose PKCα-positive cells from 6 to 9 months, whereas treated retinas had significantly higher numbers of rod bipolar cells at 9 months as highlighted by immunostaining for PKCα (Figure 4F, 4G). We did not maintain any mice for longer than 9 months since motor and behavioural skills, body weight and survival deteriorated progressively as part of the natural disease progression in *Cln6*-deficient mice[16].

7m8-mediated supplementation of CLN6 in bipolar cells specifically rescued the photoreceptor degeneration in* Cln6^{nclf} *mice

To investigate whether the transduction of bipolar cells alone was sufficient to treat the photoreceptor degeneration in *Cln6*-deficient mice, we produced two 7m8.hCLN6 vectors, one carrying the weak PCP2 promoter to drive expression in rod bipolar cells and one carrying the 4x enhanced Grm6 promoter to drive expression in all ON bipolar cells. *Cln6^{nclf}* mice at P5 or P6 received intravitreal injections with either vector at a dose of $1x10^{10}$ vg/eye. At 4 months the scotopic a-wave amplitudes were significantly higher in Grm6.hCLN6-treated retinas, reduced slightly over time but remained significantly higher up to 9 months. Retinas treated with the PCP2.hCLN6 construct showed a weaker therapeutic effect and had significantly increased scotopic a-wave amplitudes only at 6 months (Figure 5A). Figure 5B shows representative scotopic ERG

traces of a 9 months old *Cln6*^{nclf} mouse that received 7m8.Grm6.hCLN6 treatment in one eye and no treatment in the contralateral eye (see also Figure S5B, Table S3). We did not follow up on mice that received injections with 7m8.PCP2.hCLN6 for longer than 6 months in view of the limited beneficial effect. Analyses of the retinal histology showed that at 6 months hCLN6 was present in bipolar cells, rod OS had a better morphology and Mueller glia cell activation was reduced in PCP2.hCLN6- and Grm6.hCLN6-treated retinas (Figure 5C). Some ganglion cells appeared to express human *CLN6* following the administration of 7m8.Grm6.hCLN6. This was surprising because no expression of eGFP was detected in the GCL when 7m8.Grm6.eGFP was administered to wild type mice (see Figure 3D, 3E). Grm6 promoter driven expression in RGCs has been described previously[30]. A possible explanation for the preferential expression of *CLN6* over GFP in the GCL may be that the sequence of the *CLN6* transgene could contain elements that promote the 'leaky' activity of the Grm6 promoter. In agreement with the functional restoration, the thickness of the ONL was increased in both treatment groups, however this only reached significance in 7m8.Grm6.hCLN6-treated retinas with 6 rows of photoreceptor nuclei compared with 4 rows in untreated mutant retinas at 6 months (Figure 5D). No significant difference in the number of rod bipolar cells was detected following the treatment at 6 months (Figure 5E), but at 9 months the number of PKCα-positive cells was significantly increased ($p = 0.0057$) (Figure 5H) as highlighted by representative images in figure 5F. From 6 to 9 months the rows of photoreceptor nuclei remained higher in the treated eyes with 6 rows compared with 2 rows in untreated retinas ($p = 0.0025$) (Figure 5F, 5G).

Discussion

AAV-mediated gene therapies have proven a successful treatment strategy to combat photoreceptor degenerations in animal models carrying mutations in various genes[8-10]. Here, we described the development of a successful treatment for the retinal degeneration in *Cln6*-deficient mice, a model of NCL that carries a mutation in the *Cln6* gene, encoding a transmembrane ER protein of unknown function. We demonstrated that the photoreceptor degeneration in *Cln6*^{nclf} mice was amenable to treatment when the therapeutic *CLN6* transgene was delivered specifically to bipolar cells, a retinal cell type downstream of photoreceptors. The bipolar cells themselves were only lost at late disease stages after the majority of photoreceptors had died. The treatment with the ubiquitous promoter had the biggest beneficial effect, most likely because expression was achieved in all transduced bipolar cell subtypes. The administration of bipolar cell subtype-specific promoter constructs resulted in a slighter lower therapeutic effect. CLN6 deficiency in photoreceptors did not play a central role in the development or progression of the photoreceptor degeneration.

For the successful treatment of the retinal phenotype in *Cln6*^{nclf} mice, it was vital to understand the endogenous expression pattern of *CLN6* in the retina. It was surprising that *CLN6* is more highly expressed in bipolar cells than in photoreceptors since bipolars are not lost early in disease. Based on our data, a scenario could be envisaged where gene supplementation therapies targeting only the degenerating brain regions or the cell types that are lost early in the disease could be ineffective. Hence, for successful brain-directed gene therapies for CLN6 disease, variant late-infantile, it may be necessary to conduct a detailed analysis of the endogenous *CLN6* expression in the different cell types and regions of the brain. Whilst brain-directed gene therapy for

CLN6-deficiency using a ubiquitous promoter, may be successful and may not require the targeting of specific cells, there is, however, a risk that wide-spread high level non-specific expression of CLN6 may result in toxicity. The use of a specific promoter targeting the appropriate cells would decrease that risk.

Retinal disorders arising from defects in bipolar cells are rare. One such disease is complete congenital stationary night blindness (cCSNB), caused by mutations in genes expressed in bipolar cells. These lead to a complete loss of the ERG b-wave that is accurately recapitulated in mouse models harbouring mutations in genes such as *Grm6* or *Nyctalopin* (Nyx)[31,32]. AAV-mediated gene transfer to the bipolar cells of a Nyx-deficient mouse has previously been shown to partially restore bipolar cell function in this stationary disease[33]. In contrast to the phenotype observed in *Cln6*^{nclf} mice, cCSNB does not result in a severe loss of photoreceptors. To our knowledge, this is the first report to describe a retinal dystrophy in which a gene defect in bipolar cells mediates the loss of photoreceptors whilst leaving the bipolar cells largely unaffected. The ERG recordings performed in our study did not resolve whether the decrease in the scotopic b-wave in untreated *Cln6*^{nclf} mice was a result of the reduced rod photoreceptor function, an intrinsic reduction of rod bipolar cell function or a combination of both. Since the b-wave is dependent on the presence of the a-wave, it reflects photoreceptor function, synaptic transmission from photoreceptors to bipolar cells and bipolar cell function[34]. Therefore, it remains unclear whether bipolar cells, which are not lost at early disease stages in *Cln6*-deficient mice, function normally. It could be speculated that abnormal bipolar cell function could affect the function and viability of photoreceptors as these cells are metabolically very active and sensitive to intra- or

extracellular changes[35], but further studies are required to determine the disease mechanism in *Cln6*-deficient mice.

We have confirmed that in mice the intravitreal administration of the recently developed 7m8 vector in the first postnatal week led to a widespread transgene expression in all retinal layers including bipolar cells. However, larger animals such as non-human primates have a significantly thicker ILM posing a greater challenge for retinal transduction after intravitreal AAV administration. Following intravitreal injection in non-human primates, transduction by 7m8 vector appears to be limited to the fovea and retinal areas in close proximity to blood vessels[26,36], although the efficiency of bipolar cell transduction was not assessed in these studies. It thus remains to be determined whether other vectors and/or approaches are required for efficient targeting of bipolar cells in large animals and for human applications. Alternative vectors able to transduce the bipolar in the murine retina have been described, including AAV2/8BP2 and tyrosine-mutated AAVs[25,37]. However, as for AAV 7m8, the efficiency with which these vectors can transduce bipolar cells in larger animals has proved insufficient, making them less attractive for clinical use[36,37].

The ultimate aim of this study was to investigate whether gene therapy is a potential strategy to treat the retinal degeneration in CLN6 disease, variant late-infantile. As lysosomal cross-correction does not occur for CLN6, an ocular AAV-mediated treatment of *Cln6*^{nclf} mice presents a very similar challenge to deficiencies in *CLN3* or other transmembrane defects of NCL. This study therefore also provides proof-of-concept of gene therapy for CLN3 disease, juvenile, the most common form of NCL caused by a transmembrane protein defect. Of note is that once CLN3 disease patients

have lost vision it can take several years before they develop severe neurological symptoms, creating a time window for therapeutic interventions to treat the visual failure[38]. Recently, mutations in *CLN3* were also linked to cases of non-syndromic retinal degeneration in five unrelated patient families, highlighting further the need for ocular treatments for this condition[39].

Here, we established that endogenous *CLN6* is more highly expressed in bipolar cells than in photoreceptors in mouse and human retina, consistent with results from a microarray study on mouse retina[20]. The same microarray study indicates that *Cln3* is expressed in a variety of retinal cell types with a striking abundance only in microglia[20]. In a *Cln3* knock-in reporter mouse ($Cln3^{lacZ/lacZ}$) X-gal staining was present in bipolar cells as early as P14 and expression in photoreceptors became evident from P21[40]. ERG recordings in *Cln3*-deficient mice showed electronegative retinal responses with a preserved a-wave, an approximately 30 % decrease in the b-wave and no significant cell loss at 12 months[41]. *In vivo* assessment of *Cln3*-deficient mice also revealed that the GCL (including IPL and the nerve fibre layer) and the INL were significantly thinner at 18 months than in wild type mice, while the outer retina measured from OPL to OS and from the RPE to the choroid did not show any differences[42], which may indicate that morphological alterations occur only in the inner retina. In line with these findings, CLN3 disease patients present with an electronegative maximal response and only mild a-wave disturbances at the onset of the disease, pointing to an early inner retinal dysfunction[38]. Collectively, these data indicate that bipolar cells could play an important role, not only in CLN6 disease, but also in CLN3 disease. Although *CLN6* and *CLN3* encode for proteins involved in different cellular processes with different

subcellular localisation[2], the same strategy to deliver the therapeutic transgene to bipolar cells may be the key to an effective ocular treatment for both diseases.

Methods

Mice

Cln6^{nclf} mice were kindly provided by Prof. Thomas Braulke (UKE, Hamburg). C57BL/6J and PCP2.Cre mice were purchased from Harlan Laboratories (UK). PCP2.Cre mice were paired with td.tomato (flox.STOP.flox.td.tomato) mice and Cre positive litter was confirmed by genotyping. All mice were maintained under cyclic light conditions (12 h light-dark). If not further specified, the ages of adult mice ranged from 8-12 weeks. Animal experiments were performed in accordance with the ARVO Statement for the Use of Animals in Ophthalmic and Vision Research and the UK Home Office license (PPL 70/8120).

Plasmid construct

Human CLN6 (hCLN6) cDNA was cloned into a pD10 vector containing the CMV promoter. To drive expression in rod bipolar cells, the CMV promoter was replaced with the PCP2 (purkinje cell protein 2) promoter kindly provided by Prof John Oberdick (OSU, Ohio). To drive expression in all ON bipolar cells, CLN6 cDNA was cloned into the pD10 vector carrying the 4xGrm6 (4x enhanced mGluR6) promoter kindly provided by Botond Roska (FMI, Basel). To produce a null vector, the pD10 backbone was used carrying an unrelated transgene without promoter and start codon.

Production of rAAV and intraocular administration

Recombinant AAV2/8 and 7m8 vector were produced through a triple transient transfection method and purified by affinity-based AVB Sepharose column (GE Healthcare, UK) as described previously[43]. Viral particle titres were determined by

qRT-PCR using primers aligning to the SV40 poly A tail of the genomic plasmid and a specific probe carrying a FAM dye label. Viral vector administration was performed under general anaesthesia using an operating microscope (Carl Zeiss) and a 34 gauge needle (Hamilton) as described[10]. A total volume of 1.5 µl or 1 µl rAAV was injected in juvenile (P9-P10) and early postnatal (P5-P6) animals, respectively. At least two eyes were left uninjected in every mutant cohort and no animal received the same treatment in left and right eye.

Electroretinography (ERG)

ERG recordings were obtained from both eyes in mutant and wild type animals using commercially available equipment (Espion ERG Diagnosys System) as described previously[10]. After dark adaptation overnight, scotopic examinations were performed under single-flash recording using increasing light intensities. Photopic single-flash recordings were obtained following 5 minutes of light adaptation at a background light intensity of 30 cd/m^2. N represents the number of independent animal cohorts and *n* represents the number of eyes in independent animals. ERG data from the same wild type cohorts is presented in figure 2, 4, 5 to provide a reference.

Tissue preparation

Human paraffin sections of the mid-retina were provided by Dr Michael Powner (UCL, London). Institutional Review Board (IRB)/Ethics Committee approval was obtained from Dr Marcus Fruttiger (UCL, London). The tissue was fixed in 2% PFA and obtained as described previously[44]. 6 µm thick retinal sections were deparaffinised in xylene substitute (Sigma Aldrich) and rehydrated in alcohol gradients of 100%, 75%, 50% and 30% followed by a final PBS wash. For antibody staining, the slides were

heated to 120°C in 90% glyercol and 10% citrate buffer pH 6.0. For mouse retinal sections the murine eyes were enucleated following cervical dislocation and cornea, iris and lens were removed. The eye cups were fixed in 4% PFA for 1-2h, cryoprotected in 20% sucrose and flash frozen in OCT.

Immunohistochemistry

The slides were briefly washed in PBS and blocking buffer was employed containing 5% NGS, 1% BSA and 0.1% Triton-X100. The samples were incubated in primary antibody diluted in blocking buffer at 4°C overnight. Sections were washed in PBS and incubated in secondary antibody diluted in blocking buffer. Subsequently sections were washed in PBS, washed with 600nM DAPI for 5 minutes and mounted in DAKO mounting media. The slides were stored in the dark at 4°C until imaging by confocal microscopy (Leica DM5500Q).

Quantification of retinal cross sections

Eyes were sectioned in a sagittal orientation (18µm) and collected on glass slides. Confocal images (275µm x 275µm) were taken from the superior and inferior midcentral retina of three sagittal cross sections on each slide. To assess the ONL thickness, three vertical columns of DAPI-positive photoreceptor nuclei were counted in each of the six single confocal images. The counts of PKCα-positive cells were performed on the corresponding projection images. PKCα counts in figure S1 were performed on stained sections using mouse anti-PKCα antibody (Sigma Aldrich). For all other PKCα counts, staining was performed using mouse anti-PKCα antibody (Santa Cruz). Counts included age-matched wild type controls. Researchers performing counts were masked to the genotype of the animals and treatment received.

Quantitative real-time RT-PCR (qRT-PCR)

Total RNA was extracted from mouse retinas or FACS-sorted cell samples using the RNeasy® Mini Kit (Qiagen). The QuantiTect® Reverse Transcription Kit (Qiagen) was utilized to generate cDNA. qRT-PCRs were performed in 96 well plates in a PCR thermal cycler (Applied Biosciences 7900HT) using a 2x FastStart TagMan® Probe Mastermix assay (Roche) with a probe concentration of 100nm and a primer concentration of 200nm with the following primers:

forward β-actin (5'-AAGGCCAACCGTGAAAAGAT-3'),

reverse β-actin (5'-GTGGTACGACCAGAGGCATAC-3'),

forward Cln6 (5'-AGAGCCACATGCCAGGAC-3'),

reverse Cln6 (5'-GGCGAAGAAGGTGAAGATGA-3'),

forward Peripherin2 (5'-TGGATCAGCAATCGCTACCT-3') and

reverse Peripherin2 (5'-CCATCCACGTTGCTCTTGA-3'). Triplicate reactions were carried out for each sample. The Ct values were calculated using the computer programme SDS 2.2.2 (Applied Biosciences). To determine relative expression levels, the Ct values of the triplicate reactions for every gene were averaged and normalized to the averaged β-actin Ct values of each corresponding sample (ΔCt). For absolute quantification, a dilution series of plasmid DNA ranging from 1.5×10^3 to 1.5×10^7 molecules was used to produce a standard curve. A dilution series of wild type mouse retina cDNA was performed in the ratios of 1:10:100. The obtained Ct values were averaged per triplicate reaction and the number of specific cDNA molecules per nanogram total mRNA was calculated by standard curve intrapolation.

Retinal semithin sections

Eyes were enucleated, the cornea and lens removed. The eyecups were fixed in

Karnovsky fixative for least 30 hours at 4°C. The eyes were dehydrated by passage through ascending ethanol series (50-100%) and propylene oxide and infiltrated overnight with 1:1 mixture of propylene oxide: Epoxy resin. After further 8 hours in full resin, eyes were embedded in fresh resin and incubated overnight at 60°C. Semithin (0.7 µm) sections were cut in the inferior- superior axis passing through the optic nerve head using a Leica ultracut S microtome. Retinal semithin sections were stained with a 1% mixture of toluidine blue-borax in 50% ethanol. Images were captured of the inferior and superior mid-retina from three sections per eye (in total six images per eye) using a Qimaging camera (MicroPublisher 5.0 RT) mounted on a light microscope (Leica DM IRB). Images were exported as TIFFs and measurements were performed in Image J.

Fluorescence-activated cell sorting and flow cytometry analysis

Cell sorting was performed using a BD Influx Cell Sorter™ (Becton Dickinson Biosciences, USA) fitted with a 200mW 488 nm blue laser that was used to excite GFP detected in the 488-530/40nm channel, a 50mW 561 nm yellow/green laser that was used to excite tdTomato detected in the 561-585/29nm channel, and a 100mW 640nm red laser used to excite an anti-mouse CD73-APC antibody (BioLegend®, 127209) detected in the 640-670/30nm channel. Sorting of photoreceptors and bipolar cells was performed with a 70 micron nozzle at 50psi. To determine cell viability, DRAQ7™ (Biostatus, DR71000) dead cell stain was added to the samples at a final concentration of 0.6 µM for 5 minutes at room temperature. All of the samples were analysed using a BD LSRFortessa™ X-20 flow cytometer (Becton Dickinson Biosciences, USA), fitted with 5 lasers (i.e. 355nm, 405nm, 488nnm, 561nm & 640nm lasers). Results were subsequently analysed using FlowJo® software v. 9.9.5 (FlowJo, LLC).

Statistical analysis

Data are represented as means ± SD (standard deviation) or ± SEM (standard error) with the appropriate *n* (number of independent samples) values as indicated. The appropriate tests and p values are provided in the figure legends with *: $p < 0.05$, **: $p < 0.01$, ***: $p < 0.001$.

Author contributions

S.H., J.R., L.A., R.P., Y.D., A.G., R.S. and J.H. planned and conducted the experiments. S.H., R.S. and A.S. analyzed the data. R.P., Y.D., A.G., R.S., M.R., R.M., S.A., U.L., A.S., S.M. and R.A. provided expertise and feedback. A.S., S.M. and R.A. secured funding and supervised the study. S.H., A.S., S.M. and R.A. conceptualized the study and wrote the paper.

Acknowledgements

We thank Prof Thomas Braulke for the *Cln6*^{nclf} mouse line and Dr Michael Powner for providing non-diseased human retinal tissue. This project was supported by the Batten Disease Family Association, charity No 1084908, Beefy's Charity Foundation, the European Union's Horizon 2020 research and innovation programme (Grant No 66691), the European Union Seventh Framework Programme (FP7/2007–2013, Grant No 281234), RP Fighting Blindness (Grant GR576), Moorfields Eye Charity and Medical Research Council. RRA is partially supported by the NIHR Biomedical Research Centre at Moorfields Eye Hospital and the UCL Institute of Ophthalmology.

Conflict of interest

U.F.O.L. is employee of F. Hoffmann-La Roche. Ltd. The remaining authors do not declare any conflict of interest.

References:

1. Mole, S, Williams, R and Goebel, H (2011). *The Neuronal Ceroid Lipofuscinoses (Batten Disease)*. In: Mole, S, Williams, R and Goebel, H (eds.) **1**, Oxford University Press, 1pp.
2. Kollmann, K, Uusi-Rauva, K, Scifo, E, Tyynelä, J, Jalanko, A and Braulke, T (2013). Cell biology and function of neuronal ceroid lipofuscinosis-related proteins. *Biochim. Biophys. Acta* **1832**: 1866–1881.
3. Sands, M and Davidson, B (2006). Molecular Therapy - Gene Therapy for Lysosomal Storage Diseases. *Molecular Therapy* **13**: 839–849.
4. Consortium, TIBD (1995). Isolation of a novel gene underlying Batten disease, CLN3. The International Batten Disease Consortium. *Cell* **82**: 949–957.
5. Schulz, A, Kohlschütter, A, Mink, J, Simonati, A and Williams, R (2013). NCL diseases - clinical perspectives. *Biochim. Biophys. Acta* **1832**: 1801–1806.
6. Sondhi, D, Scott, EC, Chen, A, Hackett, NR, Wong, AMS, Kubiak, A, *et al.* (2014). Partial Correction of the CNS Lysosomal Storage Defect in a Mouse Model of Juvenile Neuronal Ceroid Lipofuscinosis by Neonatal CNS Administration of an Adeno-Associated Virus Serotype rh.10 Vector Expressing the Human CLN3Gene. *Human Gene Therapy* **25**: 223–239.
7. Bosch, ME, Aldrich, A, Fallet, R, Odvody, J, Burkovetskaya, M, Schuberth, K, *et al.* (2016). Self-Complementary AAV9 Gene Delivery Partially Corrects Pathology Associated with Juvenile Neuronal Ceroid Lipofuscinosis (CLN3). *Journal of Neuroscience* **36**: 9669–9682.
8. Komáromy, AM, Alexander, JJ, Rowlan, JS, Garcia, MM, Chiodo, VA, Kaya, A, *et al.* (2010). Gene therapy rescues cone function in congenital achromatopsia. *Human Molecular Genetics* **19**: 2581–2593.
9. Carvalho, LS, Xu, J, Pearson, RA, Smith, AJ, Bainbridge, JW, Morris, LM, *et al.* (2011). Long-term and age-dependent restoration of visual function in a mouse model of CNGB3-associated achromatopsia following gene therapy. *Human Molecular Genetics* **20**: 3161–3175.
10. Nishiguchi, KM, Carvalho, LS, Rizzi, M, Powell, K, Holthaus, S-MK, Azam, SA, *et al.* (2015). Gene therapy restores vision in rd1 mice after removal of a confounding mutation in Gpr179. *Nat Comms* **6**: 6006.
11. Testa, F, Maguire, AM, Rossi, S, Pierce, EA, Melillo, P, Marshall, K, *et al.* (2013). Three-Year Follow-up after Unilateral Subretinal Delivery of Adeno-Associated Virus in Patients with Leber Congenital Amaurosis Type 2. *Ophthalmology* **120**: 1283–1291.
12. Bainbridge, JWB, Mehat, MS, Sundaram, V, Robbie, SJ, Barker, SE, Ripamonti, C, *et al.* (2015). Long-term effect of gene therapy on Leber's congenital amaurosis. *N. Engl. J. Med.* **372**: 1887–1897.
13. Weleber, RG, Pennesi, ME, Wilson, DJ, Kaushal, S, Erker, LR, Jensen, L, *et al.* (2016). Results at 2 Years after Gene Therapy for RPE65-Deficient Leber Congenital Amaurosis and Severe Early-Childhood-Onset Retinal Dystrophy. *Ophthalmology* **123**: 1606–1620.
14. Ghazi, NG, Abboud, EB, Nowilaty, SR, Alkuraya, H, Alhommadi, A, Cai, H, *et al.* (2016). Treatment of retinitis pigmentosa due to MERTK mutations by ocular subretinal injection of adeno-associated virus gene vector: results of a phase I trial. *Hum. Genet.* **135**: 327–343.

15. Mole, SE, Michaux, G, Codlin, S, Wheeler, RB, Sharp, JD and Cutler, DF (2004). CLN6, which is associated with a lysosomal storage disease, is an endoplasmic reticulum protein. *Exp. Cell Res.* **298**: 399–406.
16. Bronson, RT, Donahue, LR, Johnson, KR, Tanner, A, Lane, PW and Faust, JR (1998). Neuronal ceroid lipofuscinosis (nclf), a new disorder of the mouse linked to chromosome 9 - Bronson - 1999 - American Journal of Medical Genetics - Wiley Online Library. *Am. J. Med. Genet.* **77**: 289–297.
17. Gao, H, Boustany, R-MN, Espinola, JA, Cotman, SL, Srinidhi, L, Antonellis, KA, *et al.* (2002). Mutations in a novel CLN6-encoded transmembrane protein cause variant neuronal ceroid lipofuscinosis in man and mouse. *Am. J. Hum. Genet.* **70**: 324–335.
18. Mirza, M, Volz, C, Karlstetter, M, Langiu, M, Somogyi, A, Ruonala, MO, *et al.* (2013). Progressive retinal degeneration and glial activation in the CLN6 (nclf) mouse model of neuronal ceroid lipofuscinosis: a beneficial effect of DHA and curcumin supplementation. *PLoS ONE* **8**: e75963.
19. Bartsch, U, Galliciotti, G, Jofre, GF, Jankowiak, W, Hagel, C and Braulke, T (2013). Apoptotic photoreceptor loss and altered expression of lysosomal proteins in the nclf mouse model of neuronal ceroid lipofuscinosis. *Invest. Ophthalmol. Vis. Sci.* **54**: 6952–6959.
20. Siegert, S, Cabuy, E, Scherf, BG, Kohler, H, Panda, S, Le, Y-Z, *et al.* (2012). Transcriptional code and disease map for adult retinal cell types. *Nat Neurosci* **15**: 487–495.
21. Travis, GH, Sutcliffe, JG and Bok, D (1991). The retinal degeneration slow (rds) gene product is a photoreceptor disc membrane-associated glycoprotein. *Neuron* **6**: 61–70.
22. Pawlyk, BS, Smith, AJ, Buch, PK, Adamian, M, Hong, D-H, Sandberg, MA, *et al.* (2005). Gene replacement therapy rescues photoreceptor degeneration in a murine model of Leber congenital amaurosis lacking RPGRIP. *Invest. Ophthalmol. Vis. Sci.* **46**: 3039–3045.
23. Dalkara, D and Sahel, J-A (2014). Gene therapy for inherited retinal degenerations. *Comptes Rendus Biologies* **337**: 185–192.
24. Kay, CN, Ryals, RC, Aslanidi, GV, Min, S-H, Ruan, Q, Sun, J, *et al.* (2013). Targeting photoreceptors via intravitreal delivery using novel, capsid-mutated AAV vectors. *PLoS ONE* **8**: e62097.
25. Cronin, T, Vandenberghe, LH, Hantz, P, Juttner, J, Reimann, A, Kacso, AE, *et al.* (2014). Efficient transduction and optogenetic stimulation of retinal bipolar cells by a synthetic adeno-associated virus capsid and promoter. *EMBO Molecular Medicine* **6**: 1175–1190.
26. Dalkara, D, Byrne, LC, Klimczak, RR, Visel, M, Yin, L, Merigan, WH, *et al.* (2013). In Vivo-Directed Evolution of a New Adeno-Associated Virus for Therapeutic Outer Retinal Gene Delivery from the Vitreous. *Science Translational Medicine* **5**: 189ra76–189ra76.
27. Harvey, A (2002). Intravitreal Injection of Adeno-associated Viral Vectors Results in the Transduction of Different Types of Retinal Neurons in Neonatal and Adult Rats: A Comparison with Lentiviral Vectors. *Molecular and Cellular Neuroscience* **21**: 141–157.
28. Dalkara, D, Kolstad, KD, Caporale, N, Visel, M, Klimczak, RR, Schaffer, DV, *et al.* (2009). Inner limiting membrane barriers to AAV-mediated retinal transduction from the vitreous. *Molecular Therapy* **17**: 2096–2102.

29. Oberdick, J, Smeyne, RJ, Mann, JR, Zackson, S and Morgan, JI (1990). A promoter that drives transgene expression in cerebellar Purkinje and retinal bipolar neurons. *Science* **248**: 223–226.
30. van Wyk, M, Hulliger, EC, Girod, L, Ebneter, A and Kleinlogel, S (2017). Present Molecular Limitations of ON-Bipolar Cell Targeted Gene Therapy. *Front Neurosci* **11**: 161.
31. Masu, M, Iwakabe, H, Tagawa, Y, Miyoshi, T, Yamashita, M, Fukuda, Y, *et al.* (1995). Specific deficit of the ON response in visual transmission by targeted disruption of the mGIuR6 gene. *Cell* **80**: 757–765.
32. Pardue, MT, McCall, MA, Lavail, MM, Gregg, RG and Peachey, NS (1998). A naturally occurring mouse model of X-linked congenital stationary night blindness. *Invest. Ophthalmol. Vis. Sci.* **39**: 2443–2449.
33. Scalabrino, ML, Boye, SL, Fransen, KMH, Noel, JM, Dyka, FM, Min, S-H, *et al.* (2015). Intravitreal delivery of a novel AAV vector targets ON bipolar cells and restores visual function in a mouse model of complete Congenital Stationary Night Blindness. *Human Molecular Genetics*.
34. Stockton, RA and Slaughter, MM (1989). B-wave of the electroretinogram. A reflection of ON bipolar cell activity. *J. Gen. Physiol.* **93**: 101–122.
35. Wong-Riley, M (2010). Energy metabolism of the visual system. *EB*: 99doi:10.2147/EB.S9078.
36. Ramachandran, P, Lee, V, Wei, Z, Song, JY, Casal, G, Cronin, T, *et al.* (2016). Evaluation of dose and safety of AAV7m8 and AAV8BP2 in the non-human primate retina. *Human Gene Therapy*: hum.2016.111doi:10.1089/hum.2016.111.
37. Mowat, FM, Gornik, KR, Dinculescu, A, Boye, SL, Hauswirth, WW, Petersen-Jones, SM, *et al.* (2014). Tyrosine capsid-mutant AAV vectors for gene delivery to the canine retina from a subretinal or intravitreal approach. *Gene Ther* **21**: 96–105.
38. Collins, J, Holder, GE, Herbert, H and Adams, GGW (2006). Batten disease: features to facilitate early diagnosis. *The British Journal of Ophthalmology* **90**: 1119–1124.
39. Wang, F, Wang, H, Tuan, H-F, Nguyen, DH, Sun, V, Keser, V, *et al.* (2014). Next generation sequencing-based molecular diagnosis of retinitis pigmentosa: identification of a novel genotype-phenotype correlation and clinical refinements. *Hum. Genet.* **133**: 331–345.
40. Ding, S-L, Tecedor, L, Stein, CS and Davidson, BL (2011). A knock-in reporter mouse model for Batten disease reveals predominant expression of Cln3 in visual, limbic and subcortical motor structures. *Neurobiol. Dis.* **41**: 237–248.
41. Staropoli, JF, Haliw, L, Biswas, S, Garrett, L, Hölter, SM, Becker, L, *et al.* (2012). Large-Scale Phenotyping of an Accurate Genetic Mouse Model of JNCL Identifies Novel Early Pathology Outside the Central Nervous System. In: Langmann, T (ed.). *PLoS ONE* **7**: e38310.
42. Groh, J, Stadler, D, Buttmann, M and Martini, R (2014). Non-invasive assessment of retinal alterations in mouse models of infantile and juvenile neuronal ceroid lipofuscinosis by spectral domain optical coherence tomography. *Acta Neuropathol Commun* **2**: 54.
43. Davidoff, AM, Ng, CYC, Sleep, S, Gray, J, Azam, S, Zhao, Y, *et al.* (2004). Purification of recombinant adeno-associated virus type 8 vectors by ion

exchange chromatography generates clinical grade vector stock. *J. Virol. Methods* **121**: 209–215.
44. Powner, MB, Gillies, MC, Tretiach, M, Scott, A, Guymer, RH, Hageman, GS, *et al.* (2010). Perifoveal müller cell depletion in a case of macular telangiectasia type 2. *Ophthalmology* **117**: 2407–2416.

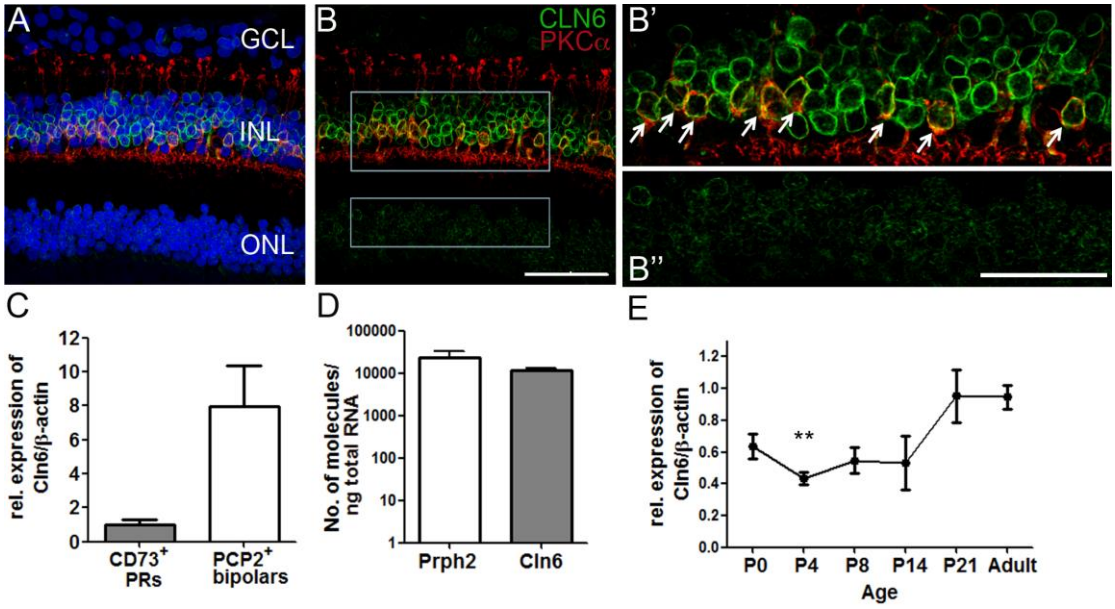

Figure 1: *CLN6* is more highly expressed in bipolar cells than in photoreceptors in human and mouse retina

Staining for CLN6 (green) and PKCα (red) on human retinal section showing high levels of CLN6 in the INL and lower levels in the ONL with (A) and without (B) DAPI nuclear counter staining in blue. Grey boxes show areas of higher magnification images. Scale bar 50µm. (B') Single confocal image revealing CLN6-positive rod bipolar cells (arrows) and (B'') CLN6-positive cells in the ONL. Scale bar 25µm. (C) *Cln6* expression level in adult mouse bipolar cells relative to photoreceptors after normalisation for ß-actin (mean ± SEM), *n* = 3 samples of 3-5 pooled retinas each (not significant, Mann-Whitney U test). (D) Absolute expression levels of *Cln6* and *Peripherin2* in adult wild type mouse retinas (means ± SEM). *Peripherin2*: *n* = 3 mice, *Cln6*^{nclf}: *n* = 4 mice. (E) Time course of the expression level of *Cln6* in wild type mouse retinas relative to adult levels, normalized for ß-actin (mean ± SEM, Kruskall-Wallis, **: $p < 0.01$ relative to P21), *n* = 2-4 mice per time point.

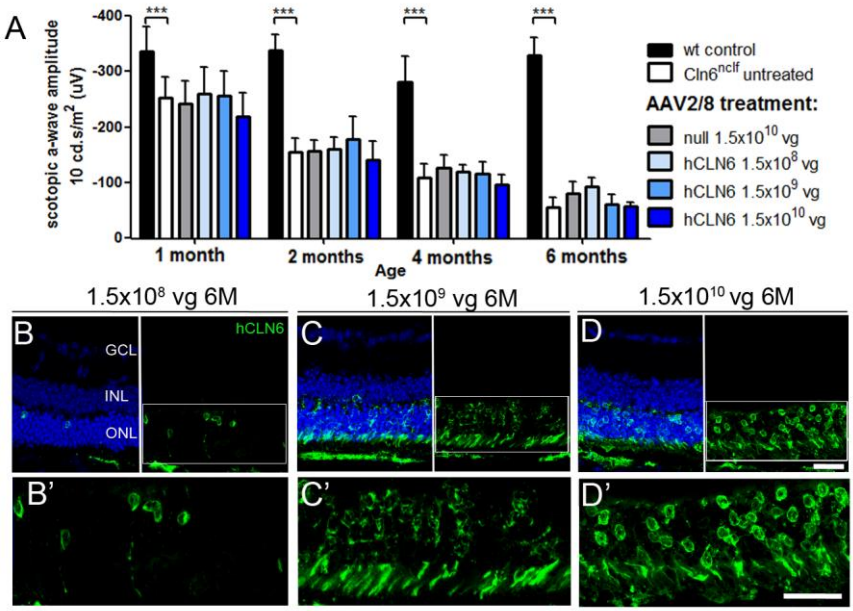

Figure 2: Subretinal delivery of AAV2/8.CMV.hCLN6 did not rescue photoreceptors in *Cln6^{nclf}* mice

(A) Scotopic ERG a-wave amplitudes of *Cln6^{nclf}* mice that received subretinal injections with AAV2/8.CMV.hCLN6 at P9-P11. Wild type: n = 5-7 eyes, N = 2; *Cln6^{nclf}* untreated: n = 14-17 eyes, N = 5; null: n = 3-4 eyes, N = 1; 1.5x10^{8} vg/eye: n = 6 eyes, N = 1; 1.5x10^{9} vg/eye: n = 7 eyes, N = 2; 1.5x10^{10} vg/eye: n = 6-8 eyes, N = 2. ***: $p < 0.001$ (2-way ANOVA-Bonferroni post-test). (B-D) hCLN6 staining confirmed transgene expression in photoreceptors at 6 months after transduction with 1.5x10^{8} vg/eye (B) and high magnification (B'), 1.5x10^{9} vg/eye (C) and high magnification (C'), 1.5x10^{10} vg/eye (D) and high magnification (D'). Scale bar 25 µm.

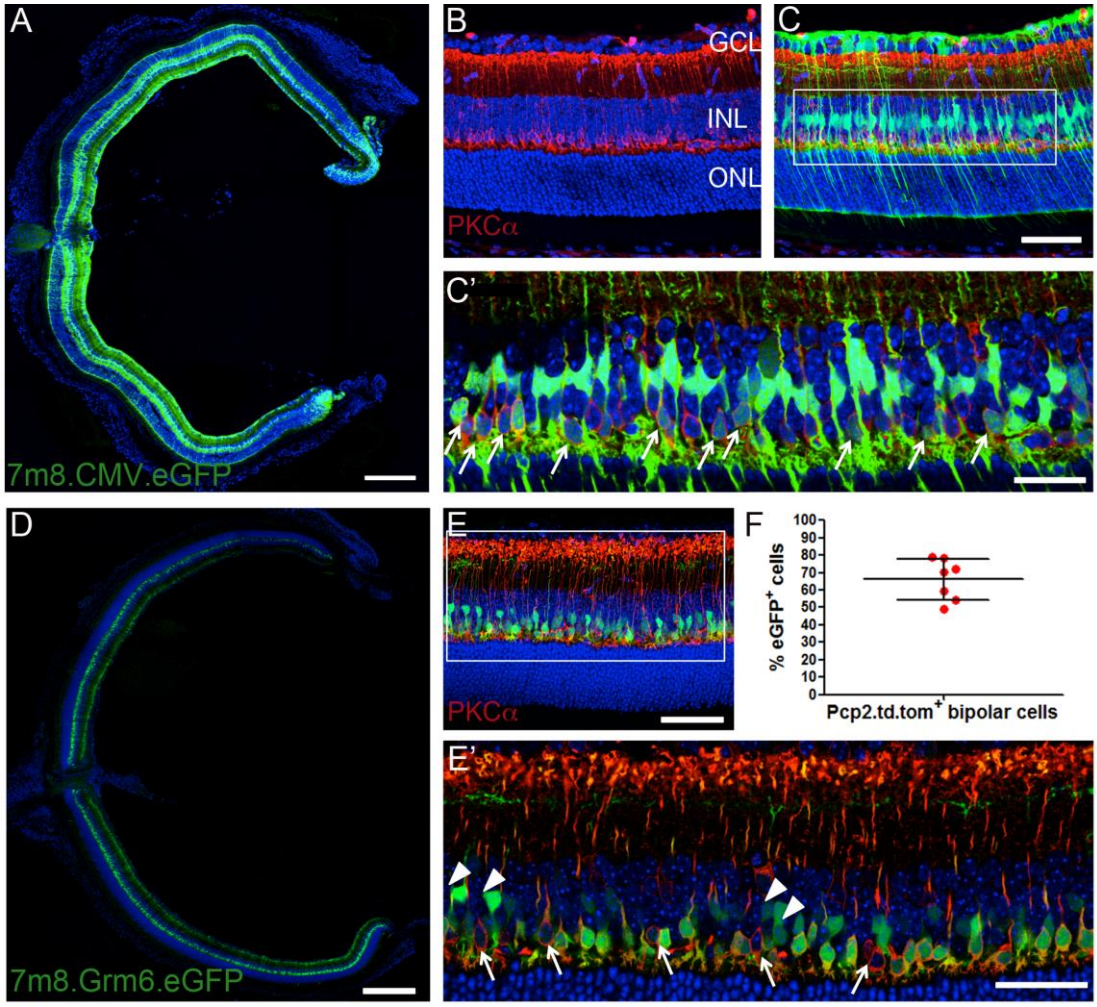

Figure 3: AAV 7m8 vector transduced mouse bipolar cells efficiently

(A) Section of wild type mouse eye 3 weeks post intravitreal injection of $1x10^{10}$ vg 7m8.CMV.eGFP at P5. Scale bar 250 μm. (B-C) Higher magnification images of wild type retinas treated with 7m8.CMV.eGFP and immunostained for PKCα (red) without (B) and with (C) the green channel shown. Scale bar 50 μm. (C') Single merged image of 7m8.CMV.eGFP-treated wild type retina showing transduced PKCα-positive rod bipolar cells. Scale bar 25 μm. (D) Section of wild type mouse eye 3 weeks post intravitreal injection of $1x10^{10}$ vg 7m8.Grm6.eGFP at P5. Scale bar 250 μm. (E) Higher magnification image of 7m8.Grm6.eGFP-treated retina stained for PKCα (red). Scale bar 50 μm. (E') Single image demonstrating transduction of the majority of PKCα-positive rod bipolar cells (arrows indicate non-transduced PKCα-positive cells) and

some cone ON bipolar cells (arrowheads), identified by the location of their cell bodies in the INL and synaptic termini in the inner plexiform layer (IPL). Scale bar 25 μm. (F) Quantification by flow cytometry of the proportion of rod bipolar cells transduced by 7m8 at P5-P6 (mean ± SD), n = 7 eyes.

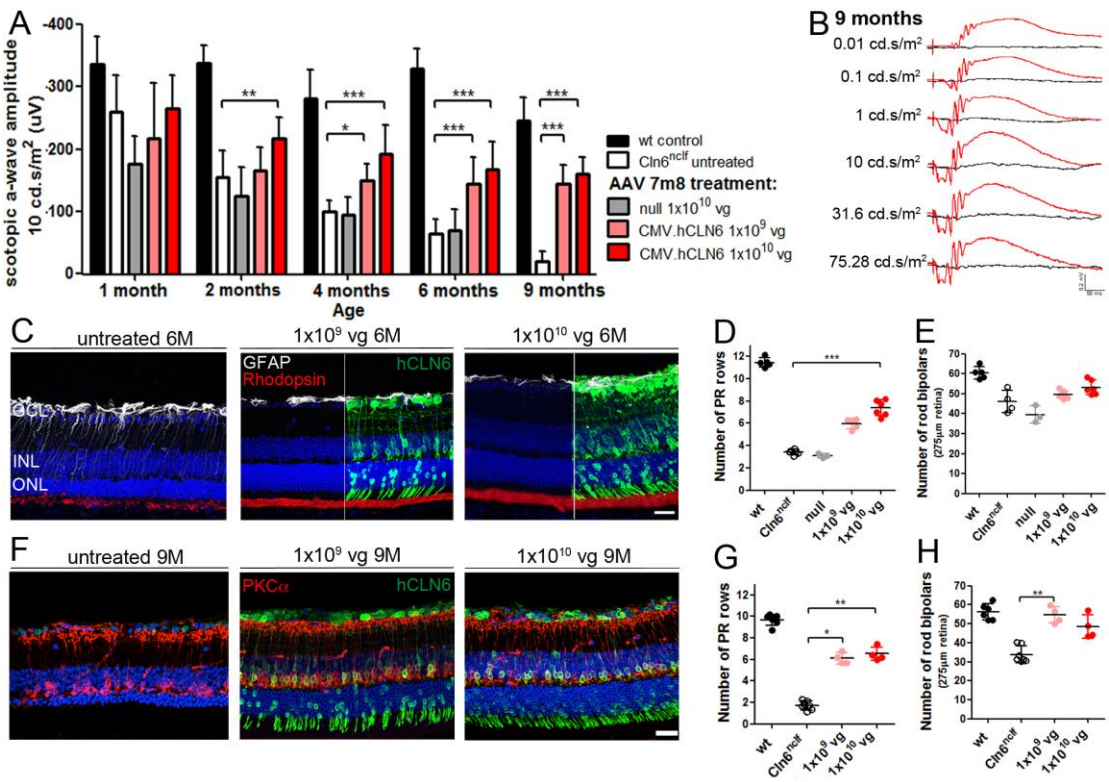

Figure 4: Intravitreal administration of 7m8.CMV.hCLN6 slowed loss of photoreceptor function and photoreceptor cells in *Cln6^{nclf}* mice

(A) Scotopic ERG a-wave amplitudes of *Cln6^{nclf}* mice after injection of 7m8.CMV.hCLN6 at P5-P6. Wild type: *n* = 5-7 eyes, N =2; *Cln6^{nclf}* untreated: *n* = 10-11 eyes (1-6 months), N = 4, *n* = 5 (9 months), N = 2; null: *n* = 3-6 eyes, N =2; 1x10^{9} vg/eye: *n* = 11-13 eyes (1-6 months), N = 4, *n* = 5 (9 months), N = 2; 1x10^{10} vg/eye: *n* = 12 eyes (1-6 months), N = 4, *n* = 4 (9 months), N =2. $p < 0.01$ = **, $p < 0.001$ = *** (2-way ANOVA-Bonferroni post-test). (B) Scotopic ERG traces of a *Cln6^{nclf}* mouse 9 months after administration of 1x10^{9} vg 7m8.CMV.hCLN6 in one eye (red). Contralateral uninjected eye in black. (C) hCLN6 staining (green) on treated and untreated eyes at 6 months. GFAP (white) and Rhodopsin (red) showed better morphology in treated eyes. (D) Quantification of photoreceptor rows and (E) PKCα-positive cells at 6 months. ***: $p < 0.001$ (Kruskal-Wallis test). (F) hCLN6 (green) and PKCα (red) staining on treated and untreated eyes at 9 months. (G) Quantification of

photoreceptor rows and (H) PKCα-positive cells at 9 months post treatment. **: $p < 0.01$, *: $p < 0.05$ (Kruskal-Wallis test). Scale bars 25 μm.

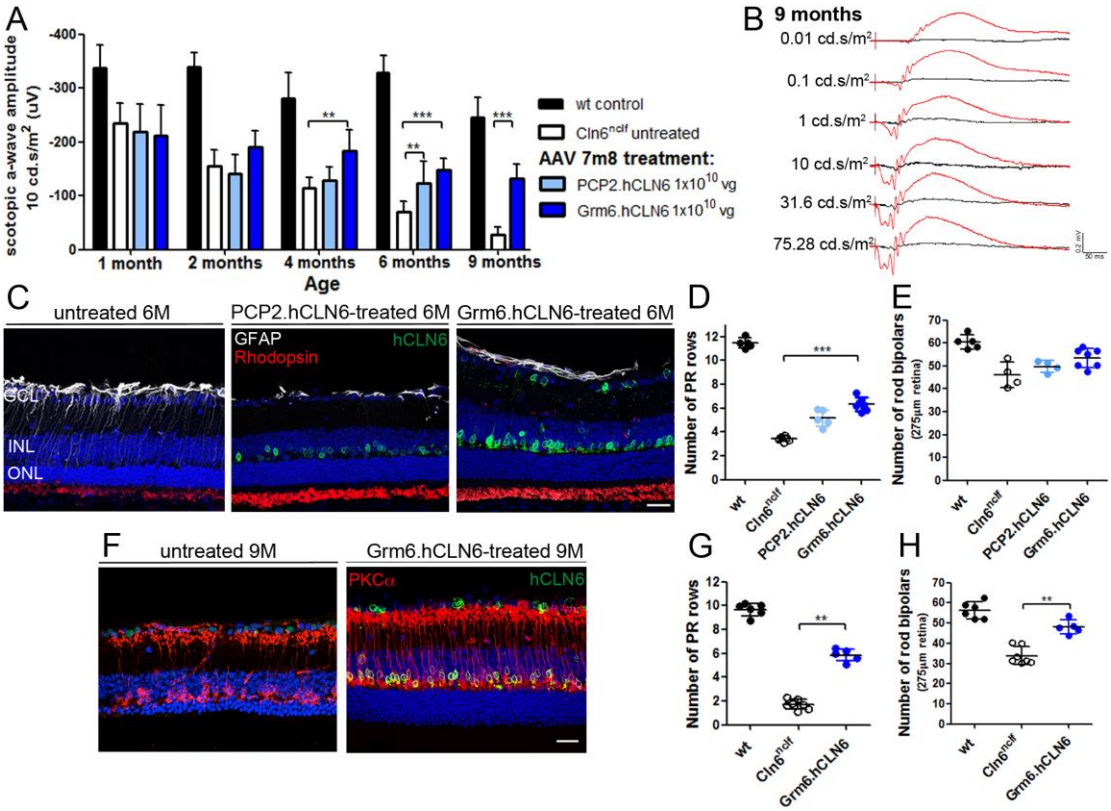

Figure 5: *hCLN6* delivery to bipolar cells slowed the loss of photoreceptor function and photoreceptor cells in *Cln6*^{nclf} mice

(A) Scotopic ERG a-wave amplitudes of *Cln6*^{nclf} mice after injection of 7m8.PCP2.hCLN6 or 7m8.Grm6.hCLN6 (1x10^{10} vg/eye) at P5-P6. $p < 0.01$ = **, $p < 0.001$ = *** (2-way ANOVA-Bonferroni post-test). Wild type: *n* = 5-7 eyes, N = 2; *Cln6*^{nclf} untreated: *n* = 7-9 eyes (1-6 months), N =3, *n* = 5 (9 months), N = 2; PCP2.hCLN6: *n* = 10-11 eyes, N = 4, Grm6.hCLN6: *n* = 14 eyes (1-6 months), N = 5, *n* = 7 (9 months), N = 3. (B) Scotopic ERG traces of a *Cln6*^{nclf} mouse 9 months after administration of 1x10^{10} vg 7m8.Grm6.hCLN6 in one eye (red). Contralateral uninjected eye in black. (C) hCLN6 staining (green) on treated and untreated eyes at 6 months confirmed transgene expression in bipolar cells. GFAP (white) and Rhodopsin (red) show better morphology in treated eyes. (D) Quantification of photoreceptor rows and (E) PKCα-positive cells, 6 months post treatment. (F) hCLN6 (green) and PKCα (red) staining on treated and untreated eyes at 9 months. (G) Quantification of

photoreceptor rows and (H) PKCα-positive cells at 9 months post treatment. **: $p < 0.01$ ***: $p < 0.001$ (Kruskal-Wallis test). Scale bars 25 μm.